American Journal of

Biochemistry and Molecular Biology

ISSN 2150-4210

Academic
Journals Inc.

www.academicjournals.com

American Journal of Biochemistry and Molecular Biology 2 (1): 30-39, 2012
ISSN 2150-4210 / DOI: 10.3923/ajbmb.2012.30.39

Nuclear Association of Nonmuscle Myosin-II within the Giant Cells of *Drosophila melanogaster* Salivary Gland Organ: Tail Domain Specifies Perinuclear Oligomerization

[1,2,3]O.W. Guthrie

[1]Research Service-151, Veterans Affairs Loma Linda Hospital, Loma Linda CA 92357, USA
[2]Department of Otolaryngology and Head and Neck Surgery, School of Medicine, Loma Linda University Medical Center, Loma Linda CA 92354, USA
[3]Department of Biology, Developmental, Cell and Molecular Biology Group, Duke University, French Family Science Center, Durham, NC 27708, USA

Corresponding Author: Dr. O.W. Guthrie, Research Service-151, Loma Linda Veterans Affairs Hospital, 11201 Benton Street, Loma Linda CA 92357, USA Tel: 909 825 7084/4533 Fax: 909 796 4508

ABSTRACT

It is know from *in vitro* experiments that contractile forces of nonmuscle myosin-II (MyoII) in the cytoplasm affect the function of the nucleus. Furthermore, perinuclear pools of MyoII have been localized among several types of cultured cells. However, beyond cell culture experiments there is no evidence that cytoplasmic MyoII associates with the nucleus. The aim of the current experiments is to determine whether or not MyoII associates with the nucleus of cells in metazoan tissue. The giant cells within salivary gland organs from 3rd instar *Drosophila melanogaster* larvae were evaluated in living and fixed preparations. A UAS-Gal4 conditional expression system was used to drive gene expression of MyoII specifically within salivary gland organs. A GFP-MyoII protein trap line which uses the endogenous MyoII promoter to control expression of full-length GFP-MyoII was also employed. Additionally, antibody immunoreactivity was used to localize endogenous MyoII proteins. The results revealed a perinuclear localization pattern for the MyoII molecule. The molecule formed oligomerized (filament-like) conformations on the cytoplasmic side of the nuclear lamin. Furthermore, the MyoII α-helical coiled-coil tail was shown to be necessary for perinuclear localization and oligomerization. These experiments provide direct evidence for a nuclear association of MyoII within metazoan tissue.

Key words: Perinuclear, protein trap, actin, Gal4, metazoan

INTRODUCTION

The nucleus can function as a mechanosensor that detects mechanical forces in the cytoplasm (Dahl *et al*., 2008). KASH (Klarsicht, ANC-1, Syne homology) proteins on the outer nuclear membrane and SUN (Sad1/UNC-84) proteins attached to nuclear lamins directly transfer force generated in the cytoplasm to the nucleus (Starr, 2009). It is known that the nucleus is sensitive to cytoplasmic forces generated by the nonmuscle myosin-II (hereafter referred to as MyoII) molecular motor. Among naïve mesenchymal stem cells, MyoII contraction affects transcriptional profiles that determine cell lineage (Engler *et al*., 2007; McBeath *et al*., 2004). Additionally, MyoII facilitates the translocation of the nucleus through the cytoplasm during interkinetic nuclear migration in the retina and nuclear positioning in the cytoplasm among migrating NIH 3T3 cells (Gomes *et al*., 2005; Norden *et al*., 2009). Furthermore, several types of cultured cells, stained with

MyoII antibodies have revealed a prominent cytoplasmic pool of MyoII around the nucleus (Hirano *et al*., 1999; Kolega, 1998; Maupin *et al*., 1994). The existence of perinuclear pools of MyoII suggest localized force generation at the nucleus. However, perinuclear pools of MyoII are also believed to serve as solatable reservoirs that are mobilized when needed by the cell. For instance, migrating bovine microcapillary endothelial cells sequester perinuclear MyoII to re-enforce a 10 μm wide region just behind their leading lamellipodia (Kolega, 1997). Additionally, during cellular locomotion a significant proportion of perinuclear MyoII from Swiss 3T3 murine fibroblast become diffusible (Kolega and Taylor, 1993). Up to 79% of the perinuclear pool of MyoII is highly diffusible while 21% exhibit a low mobility of 4.1×10^{-9} cm^2 sec^{-1} (37°C) (DeBiasio *et al*., 1988). These observations from cell culture experiments suggest that perinuclear pools of MyoII may generate force onto the nucleus and/or serve as a diffusible reservoir that reinforce tension generating loci in the cell (Engler *et al*., 2007; Kolega, 1997). However, high resolution microscopic evidence of such perinuclear reservoirs within living or fixed preparations of metazoan tissue has not been reported. Therefore, it is not clear whether the functions of perinuclear MyoII actually generalize beyond cultured cells (Norden *et al*., 2009).

In the current study living and fixed whole-mount salivary gland organs from larval *Drosophila melanogaster* were used to localize perinuclear pools of *zip*/MyoII (the *Drosophila* homolog of MyoII). These perinuclear pools exhibited an oligomerized conformation and co-distributed with filamentous actin. Furthermore, the tail domain of *zip*/MyoII was necessary for the assembly of perinuclear oligomers.

MATERIALS AND METHODS

GFP-*zip*/MyoII transgenic strains: The cloning and sequencing of GFP-*zip*/MyoII constructs into the pUAST vector and the generation of transgenic animal strains harboring UAS-GFP-*zip*/MyoII full-length or fragment have been described previously (Franke *et al*., 2005a, b). The genotypes of these and other animals used in the present study (12/06-10/09) are listed in Table 1. The UAS-Gal4 gene expression system was used to drive the expression of full-length UAS-GFP-*zip*/MyoII and UAS-GFP-*zip*/MyoII head+neck, neck+tail and tail domains in salivary glands of living *Drosophila* wandering 3rd instar larvae (review: Phelps and Brand, 1998). For instance, animals harboring full-length or domain specific UAS-GFP-*zip*/MyoII constructs were crossed with a transgenic line that harbored the salivary gland Gal4 driver (Cherbas *et al*., 2003). The GFP-*zip*/MyoII protein trap line (CC01626) which uses the endogenous *zip*/MyoII promoter to control expression of full-length GFP-*zip*/MyoII was also used in this study (Morin *et al*., 2001).

Whole-mount immunofluorescence: Wandering 3rd instar larvae were washed in dH_2O to remove adhering yeast. Salivary glands were dissected in phosphate buffered saline (PBS: 1.86 mM of NaH_2PO_4, 8.41 mM of Na_2HPO_4, 175.0 mM of NaCl, pH 7.4). The glands were then fixed in either 4% formaldehyde in PBS for 20 min, 3.7% formaldehyde in PBS for 2 h or 10% formaldehyde in PBS + 0.2% Tween for 10 min. There were no significant differences in antibody staining pattern or intensity for these fixatives, additionally, the former two fixatives preserved endogenous GFP

Table 1: Animal genotypes

Full-length *zip*/MyoII	w^{1118}; p[w+, UAST-GFP-Zipper(16.1)]/p[w+, UAST-GFP-Zipper(16.1)]
Head+neck of *zip*/MyoII	w^{1118}; p[w+, UAST-Zipper head/neck-GFP (9.3)]/ p[w+, UAST-Zipper head/neck-GFP (9.3)]
Neck+tail of *zip*/MyoII	w^{1118}; p[w+, UAST-Zipper neck/tail-GFP (5)]/ p[w+, UAST-Zipper neck/tail-GFP (5)]
Tail of *zip*/MyoII	w^{1118}; p[w+, UAST-GFP-*zip*/MyoII-Rod(ΔNterm58)(4)]/ p[w+, UAST-GFP-*zip*/MyoII- Rod(ΔNterm58)(4)]
Salivary gland driver	w^{1118}; p[Sgs3-GAL4.PD]TP1 (Bloomington stock # 6870).

fluorescence. Following fixation the salivary glands were washed 3×5 min with PT (PBS and 0.1% Triton X-100) then 30 min with PBT (PBS, 0.1% Triton X-100 and 0.1% bovine serum albumin). They were then incubated in PBT+5.0% NGS (normal goat serum) for 2 h. Primary antibodies were added to PBT+5.0% NGS at a concentration of 1: 200 and incubated over night at 4°C. The primary antibodies used in this study were anti-*Drosophila* nonmuscle MHC-656 (Kiehart and Feghali, 1986), anti-*Drosophila* nuclear lamin (Riemer *et al*., 1995), anti-*Drosophila* spectrin-243 (Thomas and Kiehart, 1994) and anti-*Drosophila* moesin (Edwards *et al*., 1997). Endogenous GFP signal was preserved throughout these procedures therefore no anti-GFP antibody was needed. Following incubation with an antibody, the salivary glands were washed 3×5 min with PBT then incubated with secondary antibody (mouse Cy3 and/or rabbit Alexa Flur 488) in PBT+NGS at a concentration of 1: 600 for 1 h at 22°C. The salivary glands were then washed 3×5 min with PBT then incubated for 1 h in a DAPI solution (10 mL of 1X PBS, 10 μL of Tween-20, 1 μL of a 20 mg mL^{-1} DAPI/H_2O solution) and/or a solution of PBT+NGS containing rhodamine phalloidin (1:600 concentration). Afterwards, the salivary glands were washed 3×5 min with PBT then incubated in mounting media (10% 1 M Tris-Cl pH 8.0, 90% glycerol, 0.5% N-propylgallate) for 15 min then mounted on glass slides. For live whole-mount immunoflurescence, wandering 3rd instar larvae were washed in dH_2O to remove adhering yeast. Salivary glands were then dissected in Schneider's *Drosophila* medium (Invitrogen Corporation, Carlsbad, CA. USA), mounted on glass slides in Schneider's *Drosophila* medium and immediately imaged.

Laser scanning microscopy (LSM): A Zeiss LSM 510 confocal on an Axio Observer microscope mounted on a motorized Marzhauser scan stage (DC 120×100 mm) was employed in these studies. The objectives used to examine salivary gland specimens were a Zeiss EC Plan-NeoFluar 40x/1.30 oil objective and a Zeiss Plan-Apochromat 100x/1.4 oil objective. The excitation wavelengths were from a 405 nm Diode laser, 488 nm Argon laser and a 561 nm Diode laser. Conventional fluorescence filters (LP420, LP505 and LP575) for DAPI, green and red were employed with pinholes ranging from 66-128 μm and optical zooms of 1.3 to 2X. Serial 3 μm Z slices were obtained throughout the salivary glands starting from the ventral most surface to the dorsum. Gain and offset were optimized for the brightest central planes of the stack. The Zeiss LSM 510 version 4.2 software was used for offline analysis of the images, such as producing Z-stacks, rotating and orienting images. Colors in a few images were sometimes modified to better convey meaning and/or contrast. For instance, DAPI-blue in some images was changed to red and green was changed to white (see caption in each image). Huygens Essential version 3.0 was used for Surface Rendering (volume visualization) in order to separate or demonstrate the association between different color volumes, such as blue-DNA, red-lamin and GFP-zip/MyoII.

RESULTS AND DISCUSSION

Perinuclear localization of *zip*/MyoII in salivary glands: Figure 1 reveals the localization of *zip*/MyoII in whole-mount salivary gland cells using three independent methods. In one method endogenous *zip*/MyoII was localized through immunolabeling with *Drosophila zip*/MyoII antibody (Kiehart and Feghali, 1986). Panels A to A" shows DAPI stained DNA (panel A), epitope immunoreactivity for *Drosophila zip*/MyoII (panel A') and a merger of the two panels (panel A"). The results reveal a prominent perinuclear pool of *zip*/MyoII. This pattern of prominent perinuclear localization is consistent with the staining pattern observed among cultured cells (Hirano *et al*., 1999; Kolega, 1998; Maupin *et al*., 1994). In the second method, GPF-*zip*/MyoII protein trap (Morin *et al*., 2001) also revealed perinuclear localization (note that in all GFP studies,

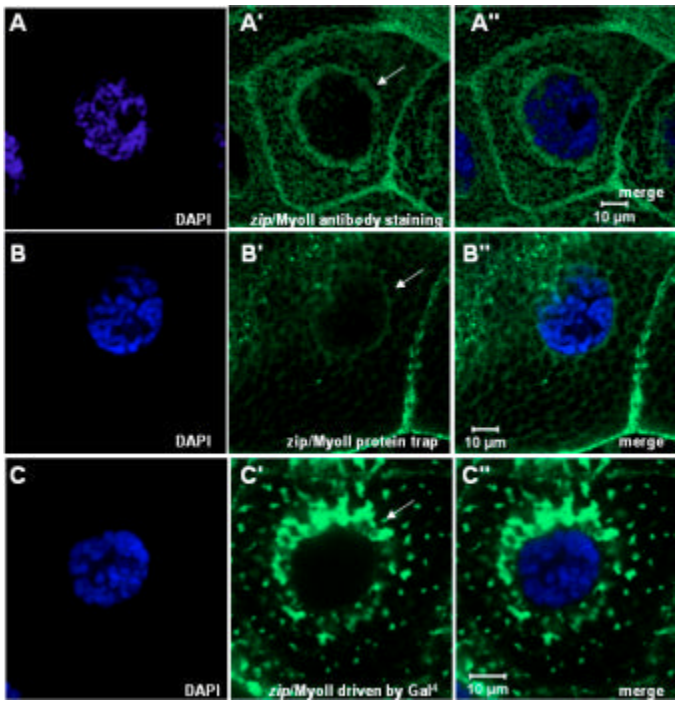

Fig. 1: Perinuclear localization of endogenous and transgenic *zip*/MyoII in single cells from whole-mount salivary gland organs. Endogenous (antibody stained) *zip*/MyoII (panels A-A") exhibit a prominent perinuclear localization. However, GFP-*zip*/MyoII protein trap (panels B-B") exhibit a modest perinuclear localization. Over-expression of GFP-*zip*/MyoII with the salivary gland specific Gal4 driver (panels C-C") result in prominent perinuclear localization. Arrows point to the perinuclear clusters of *zip*/MyoII

thendogenous GFP signal was preserved therefore, no staining was needed). Panels B to B" shows DAPI stained DNA (panel B), GPF-*zip*/MyoII fluorescence (panel B') and a merger of the two panels (panel B"). Unlike the immunolabeling method, the protein trap revealed a modest perinuclear accumulation. The third method, utilized the UAS-Gal4 expression system to over-express GFP-*zip*/MyoII (Brand and Perrimon, 1993; Franke *et al*., 2005a, b). Panels C to C" shows DAPI stained DNA (panel C), GPF-*zip*/MyoII fluorescence (panel C') and a merger of the two panels (panel C"). Similar to the immunolabeling method, the UAS-GAL4 system revealed a prominent perinuclear pool of GFP-*zip*/MyoII. This pattern of prominent perinuclear localization is consistent with the localization of GFP-MyoII among cultured cells. Furthermore, experiments where fluorescent dye labeled myosin-II is microinjected into cultured cells also reveal prominent perinuclear localization (DeBiasio *et al*., 1988; Kolega, 1998; Kolega and Taylor, 1993). Since, UAS-Gal4 expression of GPF-*zip*/MyoII (Fig. 1, panels C-C") is qualitatively similar to immunolabeling of endogenous *zip*/MyoII (Fig. 1, panels A-A"), the UAS-Gal4 expression system (Brand and Perrimon, 1993; Franke *et al*., 2005a,b) was used to further evaluate perinuclear conformations of GFP-*zip*/MyoII. Figure 2 reveals the ubiquitous nature of perinuclear pools of GPF-*zip*/MyoII by showing oligomerized conformations among each nuclei of a section of the salivary gland organ. This Fig. 2 also reveals the special distribution of GPF-*zip*/MyoII within the

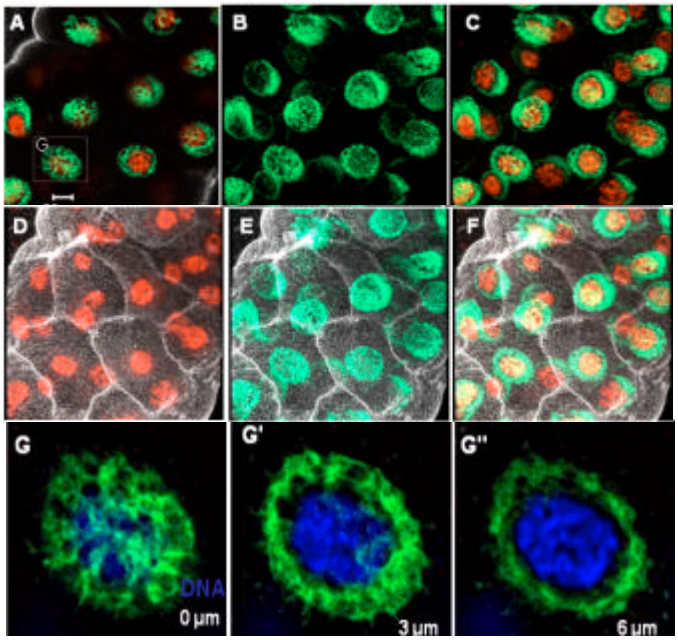

Fig. 2: Oligomerized perinuclear pools *zip*/MyoII in a whole-mount salivary gland organ. In all panels green is GFP-*zip*/MyoII, red or blue is DNA and the cell junction protein, moesin is in white. Panel A is a Z-section through a whole-mount salivary gland. Panels B-F are stacked Z-sections. Panels B-C provides a 3D view of *zip*/MyoII and DNA. Panels D-F reveal the spacial orientation of DNA and/or GFP-*zip*/MyoII within the salivary gland in general and specific cells in particular. Panels G-G" are 0-6 µm sections through the nucleus outlined in panel A

salivary gland. Furthermore, Fig. 2 provides high resolution photomicrographs of GPF-*zip*/MyoII relative to DNA. GPF-*zip*/MyoII does not seem to significantly co-localize with DNA but assemblies into oligomerized structures that spread around DNA. Furthermore, Fig. 3 shows that these oligomers are localized adjacent to the nuclear lamin on the side that is opposite to DNA (cytoplasmic side). These findings suggest that *zip*/MyoII may not directly interact with particular DNA fragments or intranuclear compartments. Instead, *zip*/MyoII may exhibit a more global influence on the nucleus. For instance, nuclear mechanosensing and transduction might be driven in part, by *zip*/MyoII mediated contractile forces in the cytosol (Engler *et al*., 2007; McBeath *et al*., 2004).

The *zip*/MyoII molecular motor is classically divided to three functionally distinct domains. There is the actin binding ATPase head domain, the light-chain regulatory neck domain and the tail domain (Franke *et al*., 2006). Individual MyoII molecules may efficiently assemble into filaments which represent the major force generating conformation (Craig and Woodhead, 2006; Liu *et al*., 2008). Filament assembly is regulated by the tail domain through hydrophobic and electrostatic interactions and phosphorylation induced mechanical folding (Hostetter *et al*., 2004; Lee *et al*., 1994; Turbedsky *et al*., 2005; Liu *et al*., 2008). It has been shown *in vitro* that the assembly of *Drosophila* zip/MyoII filaments is specifically determined by the tail domain via evenly distributed alternating charge repeats (Liu *et al*., 2008). Therefore, additional work was pursued

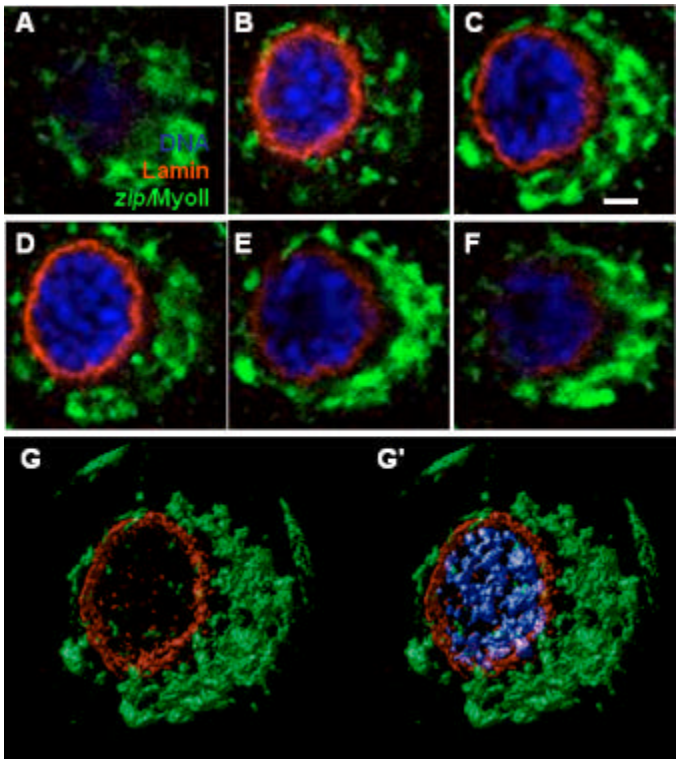

Fig. 3: *zip*/MyoII exhibits cytoplasmic perinuclear localization. Panels A-F are serial Z-zections through a single nucleus. Note that GFP-*zip*/MyoII is localized on the cytoplasmic side of the nuclear lamin (red). Panels G-G' are 3D reconstructions of panels B-F. Scale bar (10 μm) in panel C applies to all panels

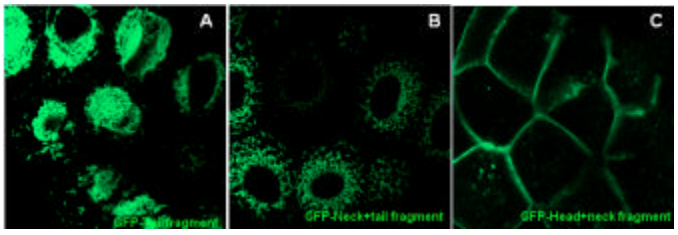

Fig. 4: *zip*/MyoII tail domain regulates the assembly of perinuclear oligomers. Panels A-C are photomicrographs of living whole-mount salivary gland organs. Note that perinuclear oligomers are observed with expression of the tail and neck+tail domains and not the head+neck domain

to determine whether or not the tail domain was responsible for specifying the assembly of perinuclear oligomers. Figure 4 reveals the expression of the tail, neck-tail and head-neck domains in living salivary gland organs. Like the antibody staining studies and the GFP tagged full length *zip*/MyoII, the tail and neck-tail constructs exhibited perinuclear oligomers. The tail formed more highly condensed perinuclear oligomers than the neck-tail construct. In contrast, the head-neck construct localized at cell borders and failed to exhibit perinuclear oligomers. This lack of

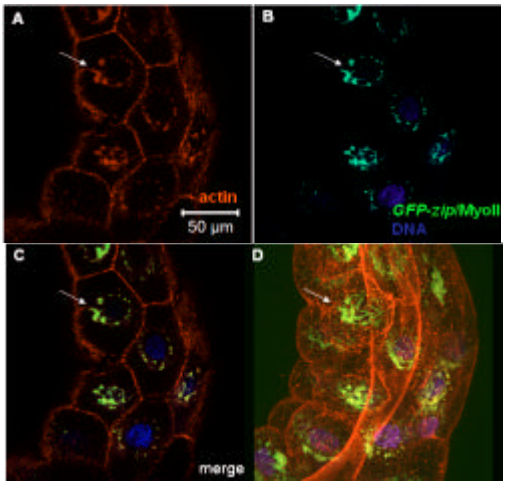

Fig. 5: *zip*/MyoII co-localize with perinuclear actin. Panel A is phalloidin stained actin in whole mount salivary gland. The arrow reveals projections from both perinuclear and cell border actin pools. Panel B is the same salivary gland showing perinuclear localization of GFP-*zip*/MyoII. Panel C is the merger of panels A and B. Note that the yellow loci reveal strong perinuclear co-localization. Panel D is the Z-stack profile of the organ

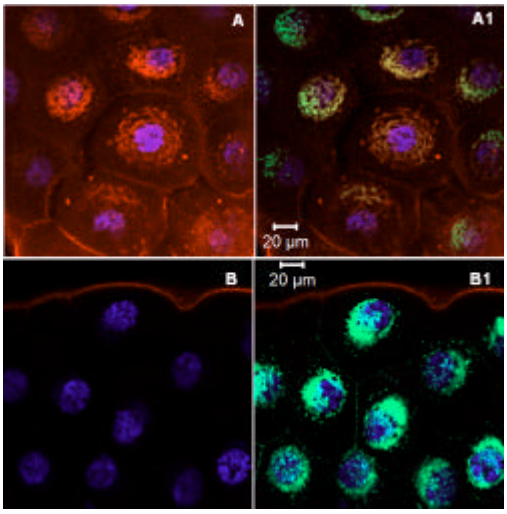

Fig. 6: Perinuclear *zip*/MyoII co-localize with some actin-binding proteins. Panel A shows that spectrin (red, antibody stain) is localized around the nucleus of salivary gland cells. Panel A1 shows the same salivary gland with co-localization of spectrin (red) and GFP-*zip*/MyoII. Note that the yellow loci are areas of strong co-localization. Panel B shows that moesin (red, antibody stain) is localized at the periphery of the salivary gland. Panel B1 shows no co-localization between GFP-*zip*/MyoII and moesin

perinuclear localization and oligomerization has been demonstrated previously for myosin-II GFP-head constructs in COS-7 cells (Ikebe *et al*., 2001).

Zip/MyoII co-localize with perinuclear actin. Actin is believed to anchor the nucleus in the cytoplasm and both actin and MyoII interact to exert tension on the nucleus (Gomes *et al*., 2005; Starr and Han, 2003). Therefore, it was suspected that GFP-*zip*/MyoII may co-localize with actin at the nucleus. Figure 5 reveals that GFP-*zip*/MyoII co-localizes with polymeric (phalloidin stained) actin around the nucleus. This actin localization pattern is similar to phalloidin labeled actin shells around the nucleus of newly divided 3T3 cultured cells (Clubb and Locke, 1998). The actin binding protein spectrin, exhibited co-localization with GFP-*zip*/MyoII in perinuclear pools. However, another actin binding protein moesin, did not co-localize with perinuclear pools of GFP-*zip*/MyoII (Fig. 6).

CONCLUSION

The existence of perinuclear pools of MyoII is well established among several types of cultured cells. In the current experiments these cell culture observations were extended by revealing perinuclear pools of MyoII in living and fixed preparations of *Drosophila* salivary gland organs. MyoII in cooperation with filamentous actin is known to generate force at the nucleus during disperate conditions such as mitosis, cellular locomotion and cell lineage determination. Among the giant nuclei of salivary gland cells both zip/MyoII and filamentous actin were localized around the nucleus which indirectly implicates a force generating capacity at the nucleus.

ACKNOWLEDGMENTS

The author would like to thank Professor Dan Kiehart for helpful comments on an earlier version of the manuscript. The lamin Dm0(ADL67.10) monoclonal antibody developed by Paul A. Fisher was obtained from the Developmental Studies Hybridoma Bank developed under the auspices of the NICHD and maintained by The University of Iowa, Department of Biology, Iowa City, IA 52242. The work was supported by the Hargitt Cell Biology Research Award.

REFERENCES

Brand, A.H. and N. Perrimon, 1993. Targeted gene expression as a means of altering cell fates and generating dominant phenotypes. Development, 118: 401-415.

Cherbas, L., X. Hu, I. Zhimulev, E. Belyaeva and P. Cherbas, 2003. EcR isoforms in *Drosopila*: Testing tissue-specific requirements by targeted blockade and rescue. Development, 130: 271-284.

Clubb, B.H. and M. Locke, 1998. Peripheral nuclear matrix actin forms perinuclear shells. J. Cell Biochem., 70: 240-251.

Craig, R. and J.L. Woodhead, 2006. Structure and function of myosin filaments. Curr. Opin. Struct. Biol., 16: 204-212.

Dahl, K.N., A.J. Ribeiro and J. Lammerding, 2008. Nuclear shape, mechanics and mechanotransduction. Circ. Res., 102: 1307-1318.

DeBiasio, R.L., L.L. Wang, G.W. Fisher and D.L. Taylor, 1988. The dynamic distribution of fluorescent analogues of actin and myosin in protrusions at the leading edge of migrating Swiss 3T3 fibroblasts. J. Cell Biol., 107: 2631-2645.

Edwards, K.A., M. Demsky, R.A. Montague, N. Weymouth and D.P. Kiehart, 1997. GFP-moesin illuminates actin cytoskeleton dynamics in living tissue and demonstrates cell shape changes during morphogenesis in *Drosophila*. Dev. Biol., 191: 103-117.

Engler, A.J., H.L. Sweeney, D.E. Discher and J.E. Schwarzbauer, 2007. Extracellular matrix elasticity directs stem cell differentiation. J. Musculoskeleton Neuronal Interact., 7: 335-335.

Franke, J.D., A.L. Boury, N.J. Gerald and D.P. Kiehart, 2006. Native nonmuscle myosin II stability and light chain binding in *Drosophila melanogaster*. Cell Motil. Cytoskeleton, 63: 604-622.

Franke, J.D., F. Dong, W.L. Rickoll, M.J. Kelley and D.P. Kiehart, 2005a. Rod mutations associated with MYH9-related disorders disrupt nonmuscle myosin-IIA assembly. Blood, 105: 161-169.

Franke, J.D., R.A. Montague and D.P. Kiehart, 2005b. Nonmuscle myosin II generates forces that transmittension and drive contraction in multiple tissues during dorsal closure. Curr. Biol., 15: 2208-2221.

Gomes, E.R., S. Jani and G.G. Gundersen, 2005. Nuclear movement regulated by Cdc42, MRCK, myosin and actin flow establishes MTOC polarization in migrating cells. Cell, 121: 451-463.

Hirano, M., N. Niiro, K. Hirano, J. Nishimura, D.J. Hartshorne and H. Kanaide, 1999. Expression, subcellular localization and cloning of the 130-kDa regulatory subunit of myosin phosphatase in porcine aortic endothelial cells. Biochem. Biophys. Res. Commun., 254: 490-496.

Hostetter, D., S. Rice, S. Dean, D. Altman and P.M. McMahon *et al*., 2004. *Dictyostelium* myosin bipolar thick filament formation: Importance of charge and specific domains of the myosin rod. PLoS Biol., 2: e356-e356.

Ikebe, M., S. Komatsu, J.L. Woodhead, K. Mabuchi and R. Ikebe *et al*., 2001. The tip of the coiled-coil rod determines the filament formation of smooth muscle and nonmuscle myosin. J. Biol. Chem., 276: 30293-30300.

Kiehart, D.P. and R. Feghali, 1986. Antibody inhibitors of nonmuscle myosin function and assembly. Methods Enzymol., 134: 423-453.

Kolega, J. and D.L. Taylor, 1993. Gradients in the concentration and assembly of myosin II in living fibroblasts during locomotion and fiber transport. Mol. Biol. Cell, 4: 819-836.

Kolega, J., 1997. Asymmetry in the distribution of free versus cytoskeletal myosin II in locomoting microcapillary endothelial cells. Exp. Cell Res., 231: 66-82.

Kolega, J., 1998. Cytoplasmic dynamics of myosin IIA and IIB: Spatial sorting of isoforms in locomoting cells. J. Cell Sci., 111: 2085-2095.

Lee, R.J., T.T. Egelhoff and J.A. Spudich, 1994. Molecular genetic truncation analysis of filament assembly and phosphorylation domains of Dictyostelium myosin heavy chain. J. Cell Sci., 107: 2875-2886.

Liu, S.L., N. Fewkes, D. Ricketson, R.R. Penkert and K.E. Prehoda, 2008. Filament-dependent and independent localization modes of *Drosophila* non-muscle myosin II. J. Biol. Chem., 283: 380-387.

Maupin, P., C.L. Phillips, R.S. Adelstein and T.D. Pollard, 1994. Differential localization of myosin-II isozymes in human cultured cells and blood cells. J. Cell Sci., 107: 3077-3090.

McBeath, R., D.M. Pirone, C.M. Nelson, K. Bhadriraju and C.S. Chen, 2004. Cell shape, cytoskeletal tension and RhoA regulate stem cell lineage commitment. Dev. Cell, 6: 483-495.

Morin, X., R. Daneman, M. Zavortink and W. Chia, 2001. A protein trap strategy to detect GFP-tagged proteins expressed from their endogenous loci in *Drosophila*. Proc. Natl. Acad. Sci. USA., 98: 15050-15055.

Norden, C., S. Young, B.A. Link and W.A. Harris, 2009. Actomyosin is the main driver of interkinetic nuclear migration in the retina. Cell, 138: 1195-1208.

Phelps, C.B. and A.H. Brand, 1998. Ectopic gene expression in *Drosophila* using GAL4 system. Methods, 14: 367-379.

Riemer, D., N. Stuurman, M. Berrios, C. Hunter, P.A. Fisher and K. Weber, 1995. Expression of *Drosophila* lamin C is developmentally regulated: Analogies with vertebrate A-type lamins. J. Cell Sci., 108: 3189-3198.

Starr, D.A. and M. Han, 2003. ANChors away: An actin based mechanism of nuclear positioning. J. Cell Sci., 116: 211-216.

Starr, D.A., 2009. A nuclear-envelope bridge positions nuclei and moves chromosomes. J. Cell Sci., 122: 577-586.

Thomas, G.H. and D.P. Kiehart, 1994. Beta heavy-spectrin has a restricted tissue and subcellular distribution during *Drosophila* embryogenesis. Development, 120: 2039-2050.

Turbedsky, K., T.D. Pollard and M. Yeager, 2005. Assembly of *Acanthamoeba* myosin-II minifilaments. Model of anti-parallel dimers based on EM and X-ray diffraction of 2D and 3D crystals. J. Mol. Biol., 345: 363-373.